Robust doped-$BaCeO_{3-\delta}$ Electrolyte for IT-SOFCs

M. Naeem Khan[1,2], A.K. Azad[1,3], C.D. Savaniu[4], Peter Hing[1], J.T.S. Irvine[4]

[1]Centre of Advanced Materials and Energy Sciences, Universiti Brunei Darussalam, Jalan Tunku Link, Gadong BE 1410, Brunei Darussalam

[2]Department of Physics, Faculty of Arts and Basic Sciences, Balochistan University of Arts and Basic Sciences, Quetta, Baluchistan, Pakistan

[3]Faculty of Integrated Technologies, Universiti Brunei Darussalam, Jalan Tunku Link, Gadong BE 1410, Brunei Darussalam

[4]Centre for Advanced Materials, School of Chemistry, University of St Andrews, Fife KY16 9ST, UK

Corresponding author: Email: abul.azad@ubd.edu.bn; Phone: +6737219025

ABSTRACT

Single phase polycrystalline $BaZr_{0.3}Ce_{0.5}Y_{0.1}Yb_{0.1}O_{3-\delta}$ electrolyte material was prepared by solid state reaction route. Rietveld analysis of the XRD data confirms the tetragonal symmetry in the I4/mcm space group with unit cell parameters of $a = b = 6.0567(3)$ Å and $c = 8.5831(5)$ Å. The addition of ZnO as a sintering additive was found to reduce the sintering temperature and enhance both overall sinterability and grain growth. Sintering temperature was reduced by 200 – 300ºC and a very high relative density of about 98% was achieved at 1400 ºC. Impedance spectroscopy in humidified 5% H_2/Ar atmosphere shows that the protonic conductivity at 600 ºC was 8.60×10^{-3} S cm^{-1}. Thermal analysis performed in pure CO_2 atmosphere shows very good chemical stability up to 1200 ºC. Good biaxial flexure strength of 100 – 200 MPa was reported which makes this material a promising electrolyte material for intermediate temperature solid oxide fuel cells (IT-SOFCs).

Keywords: perovskites, proton conductor, SOFC, electrochemical characterization, crystal structure

1. Introduction

Perovskite structured high temperature proton conducting oxides have attracted great attention due to **their** potential applications in solid oxide fuel cells, hydrogen sensors, hydrogen and water vapour pumps, high temperature ceramic reactors, etc. [1]–[5]. Solid Oxide Fuel Cells (SOFCs) with proton conducting electrolytes operates in the intermediate temperature (400 – 700 ºC) range due to lower activation energy required for the transport of protonic defect (i.e. in the range 0.30 - 0.60eV), which is much lower than the activation energy required for oxide-ion conduction (i.e. around 1.10eV) [6]. **There are many advantages of employing intermediate temperature solid oxide fuel cells (IT-SOFCs) over conventional high temperature solid oxide fuel cells (HT-SOFCs) including relatively cheap materials, easier and more reliable sealing, short start-up and shut-down time, negligible electrode sintering and less chances of materials degradation** [7]. Also fuel dilution is avoided due to water formation at the cathode side and hence complete utilization of fuel can be carried out.

Since Iwahara and co-workers [8] discovered protonic conductivity in 1981, doped-$BaCeO_3$ and doped-$BaZrO_3$ have been extensively investigated as electrolyte materials for intermediate temperature solid oxide fuel cells (IT-SOFCs) [6]. Doped $BaCeO_3$ e.g. $BaCe_{0.9}Y_{0.1}O_{3-\delta}$ possess sufficient ionic conductivity for practical applications at intermediate temperature range but its chemical stability in CO_2 and in water containing atmospheres is poor [9], [10]. On the other hand, doped $BaZrO_3$ e.g. $BaZr_{0.9}Y_{0.1}O_{3-\delta}$ possess excellent stability in CO_2 and H_2O containing atmospheres but their ionic conductivity is not **adequate** for practical applications [11]. As there is a trade-off relation between conductivity and chemical stability, solid solutions between $BaCeO_3$ and $BaZrO_3$ have been proposed and one solid solution i.e. $Ba(Zr_{0.1}Ce_{0.7}Y_{0.2})O_{3-\delta}$ has been reported to possess the highest ionic conductivity of 9×10^{-3} at 500 ºC and showed excellent chemical stability in 2% CO_2 atmosphere at 500 ºC (kept for one week) and also good stability in H_2O vapour atmosphere [12]. However later on it was reported that $Ba(Zr_{0.1}Ce_{0.7}Y_{0.2})O_{3-\delta}$ (BZCY) was not stable even in mild conditions of only 3% CO_2 at 600 ºC for 24 hours [13]. Recently $BaZr_{0.1}Ce_{0.7}Y_{0.1}Yb_{0.1}O_{3-\delta}$ (BZCYYb) has been reported to possess higher conductivity [14]–[16] and better stability than BZCY but, later, it has also been reported that it was not stable in CO_2/N_2 (1:2 ratio) when heated up to 800 ºC and then cooled down at 10 ºC/min [17].

In order to enhance chemical stability, usually the ratio of Zr is increased in $BaCeO_3$ and $BaZrO_3$ solid solutions. However, an increase of Zr content causes a decrease in ionic conductivity and further increase in sintering temperature, usually in the range 1700 – 1800 ºC, which is much higher than the co-sintering temperature of anode and electrolyte bi-layers [18]. Even for proton conducting oxides with less amount of zirconia like $Ba(Zr_{0.1}Ce_{0.7}Y_{0.2})O_{3-\delta}$ and $BaZr_{0.1}Ce_{0.7}Y_{0.1}Yb_{0.1}O_{3-\delta}$, sintering temperature of 1550ºC is required to get a densification of > 90% when processed by solid state route

[11], [13]. So in order to address the issue of poor sinterability, various sintering additives e.g. Al_2O_3, MgO, Y_2O_3, NiO, CuO, ZnO, Na_2CO_3, LiF, MnO, Fe_2O_3, Co_3O_4 [14], [19]–[24] have been reported in the literature. However ZnO was found to be good and it was observed that it was not only an effective sintering additive but also beneficial in growing grains of relatively uniform size [20]. Tao and Irvine reported that ZnO doping reduced the sintering temperature as well as enhanced its chemical stability and the composition with 4 mol% ZnO doping at the B site i.e. $BaCe_{0.5}Zr_{0.3}Y_{0.2}Zn_{0.04}O_{3-\delta}$ was much more stable than without ZnO i.e. $BaCe_{0.5}Zr_{0.3}Y_{0.2}O_{3-\delta}$, without impairment of ionic conductivity [22]. Zhang et al. [19] reported that by ZnO addition to $Ba_{1.03}Ce_{0.5}Zr_{0.4}Y_{0.1}O_{3-\delta}$ **they** achieved good densification along with an enhancement of chemical stability and grain boundary conductivity. Azad and Irvine showed that highly dense $BaCe_{0.5}Zr_{0.35}Sc_{0.1}Zn_{0.05}O_{3-\delta}$ material can be prepared **at** low temperature through ZnO doping [25].

Here, in this work, ZnO has been added to a new composition $BaZr_{0.3}Ce_{0.5}Y_{0.1}Yb_{0.1}O_{3-\delta}$ as sintering additive and its structure, densification**,** conductivity, stability and mechanical strength have been investigated. We report the stability in CO_2 atmosphere and the achievement of high protonic conductivity by doping 10% Yb with balancing 50% Ce, 30% Zr and 10% Y at the B-site. Yb with smaller ionic radius (0.868Å) than Y^{+3} (0.90Å) is added to enhance the chemical stability in acidic gases like CO_2, which is one of big challenge in the employment of proton conducting oxides. It is a well-documented fact that doping of smaller ionic radius at the B-site enhances chemical stability of Ba-based cerates-zirconates solid solutions [26]. We also report the low temperature densification (1400 ^oC) by adding 1 wt % ZnO as sintering aid. We report mechanical strength measurement and its Weibull moduli for the first time for proton conducting oxides up to the best of our knowledge.

2. Experimental

$BaZr_{0.3}Ce_{0.5}Y_{0.1}Yb_{0.1}O_{3-\delta}$ (BZ3C5YYb) powders were synthesized via conventional solid state reaction (SSR) method. Stoichiometric amounts of $BaCO_3$ (Analar), CeO_2 (Aldrich), ZrO_2 (Acros Organics), Y_2O_3 (Alfa Aesar) and Yb_2O_3 (Alfa Aesar) were mixed together and milled for 48 hours in roller ball mill in the presence of ethanol using zirconia as a milling media. After milling, the slurry was dried on a hot plate at 80 ºC for 24 hours and then it was pelletized by uni-axial press and calcined at 1400 ºC for 10 hours in air. After calcination, the sample was ground using mortar and pestle and then planetary ball milled for 2 - 3 hours, dried and calcined again for the 2nd time under the same conditions.

X-ray diffraction data was collected using a PANalytical Empyrean Diffractometer also operated in reflection mode to identify the phase, index the pattern and do Rietveld refinement. The sample was scanned from 10 - 90º 2θ for 8 hours with a step size of 0.02º. The high resolution XRD patterns were analysed through the Rietveld method by using the Fullprof software [27] in order to extract information regarding unit cell parameters, atomic positions and oxygen occupancy. Dilatometry of the sample **was**

carried out via NETZSCH DIL 402C dilatometer. First 1 wt. % of ZnO sintering additive was added to already calcined sample and was milled for 24 hours in ethanol using zirconia as milling media. The slurries were dried at 80 ºC for 24 hours and then pressed into cylinders with 13mm diameter by uniaxial compaction. The as-pressed green pellets were put in dilatometer and heated up to 1450 ºC with a heating rate of 3 ºC/min, held isothermally for 30 minutes, and then cooled down to room temperature with the cooling rate of 3 ºC/min.

Microstructure was analysed using JEOL 5600 SEM. The pellets were pressed under the same conditions as for dilatometry, and then sintered at 1400 ºC for 3 hours before taking the SEM image from the surface of the pellet samples. A sputtering device was used to sputter gold on the surface of the pellets to reduce the charge accumulation during the experiments. Relative density of the sintered pellets was measured with the help of helium gas pycnometer.

Ionic conductivity of the sample was measured by an AC method using a Schlumberger Solartron 1255 frequency response analyser coupled with a 1287 electrochemical interface controlled by Zplot electrochemical impedance software. The sintered pellet was polished, silver painted, dried in the oven and then fired at 600 ºC for 30 minutes. Then Impedance was measured in the temperature range 100 – 750 ºC in wet 5 vol% H_2/Ar atmosphere in the frequency range of 1MHz – 10mHz and an amplitude of 50mA was applied.

Chemical stability of the samples was tested using Thermogravimetric analyzer. The ground sample after sintering was heated in pure CO_2 up to 1200 ºC with a heating rate of 3 ºC/min, held isothermally for 30 minutes, and then cooled down to room temperature with the same rate of 3 ºC/min.

Bi-axial flexure strength was measured via a compaction-type test machine Lloyd LRX -05 fitted with a 500N load cell. In this study, 15 specimens in the form of cylinders with 27 mm diameter were pressed by uniaxial press for two samples i.e. ZnO-added $BaZr_{0.1}Ce_{0.7}Y_{0.1}Yb_{0.1}O_{3-\delta}$ and ZnO-added $BaZr_{0.3}Ce_{0.5}Y_{0.1}Yb_{0.1}O_{3-\delta}$ and sintered at 1400 ºC, for 3, 3 hours in air. The specimen in cylindrical shape after sintering was placed on three symmetrical bearing and some load is applied. The force is applied at the centre of the pellet (cylindrical shape) though an upper flat perpendicular to the specimen at a constant rate until the specimen breaks and the applied load at which the specimen breaks, is recorded. Weibull moduli **were** also plotted for both samples.

3. Results and Discussion

3.1. Phase Analysis

$BaZr_{0.3}Ce_{0.5}Y_{0.1}Yb_{0.1}O_{3-\delta}$ was calcined two times at 1400 ºC to get a pure single phase material. Figure 1 shows the X-ray diffraction pattern of BZ3C5YYb at room temperature. The powdered sample was scanned with a step angle of 0.02º for 8 hours in the 2θ angle range 10 – 90º for Rietveld refinement. The lattice of $BaZr_{0.3}Ce_{0.5}Y_{0.1}Yb_{0.1}O_{3-\delta}$ was found to possess tetragonal symmetry with space group I4/mcm. The lattice parameters were found to be; $a = b = 6.0567(3)$Å and $c = 8.5831(5)$ Å with unit cell volume as 314.85(3)Å^3 as shown in table 1. However these values slightly differ from those recently reported by Shi et al. **who** investigated the $BaZr_{0.3}Ce_{0.5}Y_{0.2-x}Yb_xO_{3-\delta}$ system and for x = 0.1 i.e. $BaZr_{0.3}Ce_{0.5}Y_{0.1}Yb_{0.1}O_{3-\delta}$ reported an orthorhombic symmetry after calcination at 1050 ºC for 3 hours, synthesized via citrate-nitrate process [16]. Their reported lattice parameters were a = 6.1033Å, b = 6.0992Å and c = 8.6736Å which unit cell volume = 322.88Å^3. The difference in symmetry might be due to the change in processing route and sintering temperature or indeed moisture content.

In fact, symmetry and cell parameters can be different in multiple doped $BaCeO_3$ depending on their B-site cation ratios, synthesis route and final sintering temperature. Katahira et al. [18], while studying $BaCe_{0.9-x}Zr_xY_{0.1}O_{3-\delta}$ system processed by solid state route, reported orthorhombic symmetry for x = 0, 0.05, 0.15, 0.2, and cubic symmetry for x = 0.30, 0.50, 0.90. Fabbri et al. [28] investigated the system $BaCe_{0.8-x}Zr_xY_{0.2}O_{3-\delta}$ processed by sol-gel route and reported orthorhombic structure for x = 0, 0.3, 0.5 and cubic structure for x = 0.8. Guo et al. [29] processed the system $BaZr_yCe_{0.8-y}Y_{0.2}O_{3-\delta}$ by sol-gel route and reported orthorhombic symmetry for y = 0.10 – 0.50 and cubic symmetry for y = 0.60, 0.70, 0.80. Recently, Sawant et al. [30] processed the composition $BaCe_{0.8-x}Zr_xY_{0.2}O_{3-\sigma}$ by solid state route and reported orthorhombic structure for x = 0 and cubic structure for x = 0.2, 0.4, 0.6 and 0.8. For example, $BaZr_{0.3}Ce_{0.5}Y_{0.2}O_{3-\delta}$ is orthorhombic [28], [29] when synthesized via sol-gel process; while cubic [30] when processed via solid state route. Also for one similar composition i.e. $BaCe_{0.6}Zr_{0.3}Y_{0.1}O_{3-\delta}$ cubic symmetry has been reported when processed via solid state route. These studies show the influence of the preparation procedure and sintering temperatures involved for obtaining the materials onto their crystalline structure. Higher calcination temperature, normally used for solid state reaction, might have important effect in changing the symmetry in the crystal structure. In the process of structure refinement, we have tried with orthorhombic, tetragonal and cubic symmetry. We have found the tetragonal structure with I4/mcm space group gives the best R-factors with best matching Bragg peaks.

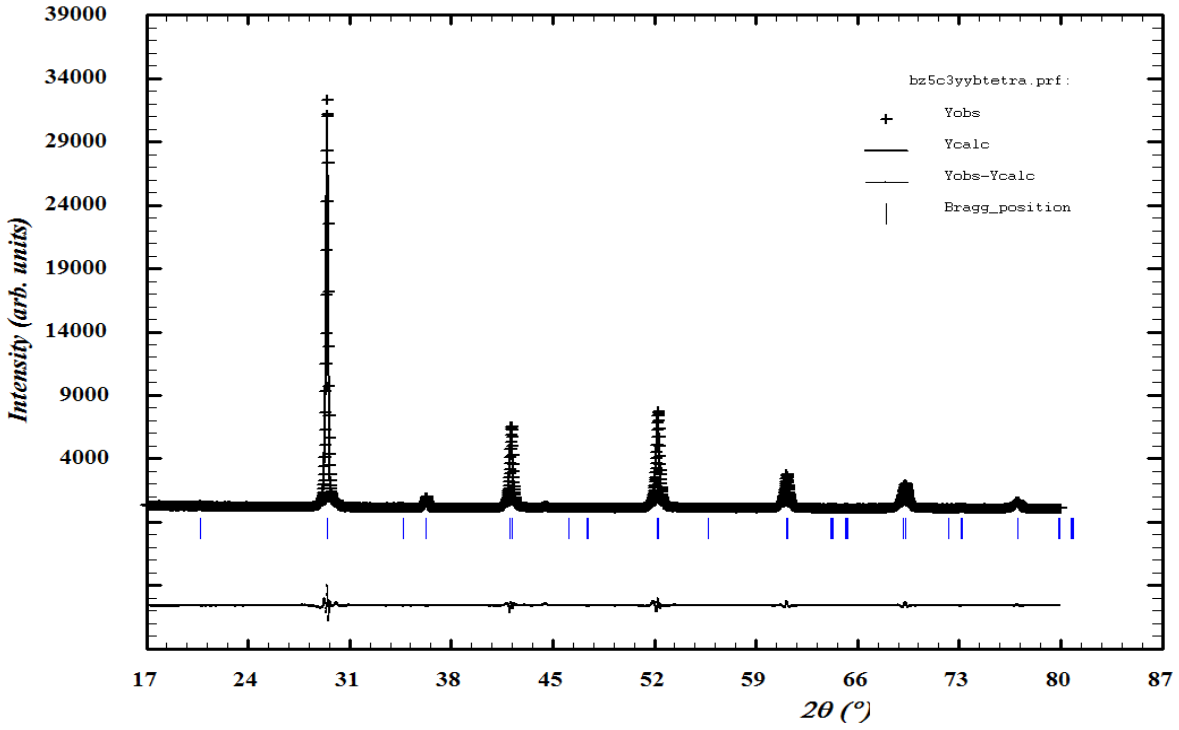

Fig.1. Rietveld refinement profile of X-Ray diffraction data of $BaZr_{0.3}Ce_{0.5}Y_{0.1}Yb_{0.1}O_{3-\delta}$. Difference ($Y_{obs}$-$Y_{cal}$) line is the bottom one of the graph.

Table 1: Summary of the Rietveld refinement results for $BaZr_{0.3}Ce_{0.5}Y_{0.1}Yb_{0.1}O_{3-\delta}$ processed via solid state route

Symmetry	Tetragonal
Space group	I4/mcm
Cell parameters (Å)	a = b = 6.0567(3), c = 8.5831(5)
Cell volume (Å^3)	314.85(3)
Oxygen occupancy	88%
Overall temperature factor	2.76(3)
R-factors (%)	R_p = 6.74, R_{wp} = 9.15, R_{exp} = 5.14, R_B = 1.24
χ^2	3.17

3.2. Sinterability

Poor sinterability of proton conducting electrolyte materials is one **of** the main challenges in the development of proton conducting solid oxide fuel cells (H-SOFCs). In $BaCeO_3$ – $BaZrO_3$ solid solutions, the sinterability further decreases with increase in zirconia content. Guo et al. [29] reported a drop in linear shrinkage as well as in relative density with increasing y i.e. zirconia content in $BaZr_yCe_{0.8-y}Y_{0.2}O_{3-\delta}$ system . This also shows that there is direct relation between shrinkage and relative density. Even when processed by wet chemical route, which reduces the sintering temperature, still ~1600 ^oC is required to get a densification to > 90%, which is much higher than co-sintering temperature of anode-

electrolyte bi-layers [28]. High temperature sintering for **a** long time causes Ba loss, which results in consumption of hydroxyl vacancies [$(OH)_O^{\bullet}$] and consequently reduces the total ionic conductivity [31]. That is one of the motivations for adding a sintering additive ZnO to help with the material densification in this work.

Sintering behaviour of 1 wt. % ZnO-added $BaZr_{0.3}Ce_{0.5}Y_{0.1}Yb_{0.1}O_{3-\delta}$ was studied and the dilatometry results are shown in Fig. 2. First derivative of sinterability curve is to know the temperature of maximum shrinkage rate as shown by dotted line in Fig. 2. Shrinkage starts at ~ 866.90 ºC and reaches to its maximum value at 1271.70 ºC as evident from Fig. 2. A quite significant shrinkage of 19.45% was achieved which is higher than reported shrinkage of 15.17% for 4 mol% ZnO composition i.e. $BaC_{0.5}Zr_{0.3}Y_{0.16}Zn_{0.04}O_{3-\delta}$ [22]. For $BaZr_{0.3}Ce_{0.5}Y_{0.2}O_{3-\delta}$ when processed by wet chemical route, a shrinkage of 14.27% has been reported [29]. **In this work** the sintering temperature has been reduced by 200 – 300 ºC and a very high relative density of about 98% has been achieved.

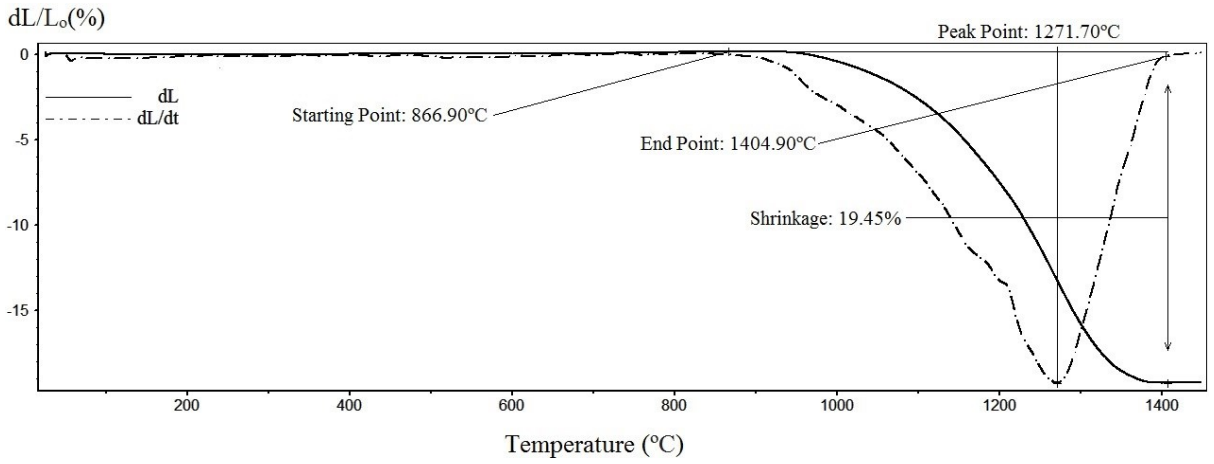

Fig.2. Sinterability studies of 1 wt. % ZnO-added $BaZr_{0.3}Ce_{0.5}Y_{0.1}Yb_{0.1}O_{3-\delta}$ heated up to 1450 ºC in dilatometry, the dotted line represents the first derivative.

3.3. Microstructure

Microstructure **plays** a very important role on the properties of the material and even more important in the case of the fuel cell electrolytes that need to be gas tight to prevent the mixing of gaseous reactants**. Grain boundary resistance is detrimental to total conductivity and an increase in grain size reduces number density of grain boundaries, which results in reduction of grain boundary resistance but may make it weaker.**

Fig. 3 shows the surface morphologies of 1wt. % ZnO-added $BaZr_{0.3}Ce_{0.5}Y_{0.1}Yb_{0.1}O_{3-\delta}$ studied via JEOL 5600 SEM. The microstructure is quite dense as evident from Fig. 3 (a) and (b). Generally grain growth increases with increase in sintering temperature and duration. The grains are rounded in shape,

with a relatively wide distribution in the range 1 – 10 μm which is in the same range with the grain size distribution of 2 – 8 μm reported for pure $BaCe_{0.5}Zr_{0.3}Y_{0.2}O_{3-\delta}$, after sintering at 1600 ºC for 8 hours [28]. The average grain size is ~ 4 – 5μm which is bigger than reported average grain size for $BaCe_{0.45}Zr_{0.45}Y_{0.1}O_{3-\delta}$, which was 3 – 4μm after sintering at 1600 ºC for 10 hours [32]. Guo et al. reported a grain size in the range 0.6 – 1.0 μm for ZnO-added $BaZr_{0.4}Ce_{0.4}Y_{0.2}O_{3-\delta}$ sample fired at 1200 ºC for 5 hours [33]. A grain size > 1.5μm was reported for ZnO-added (1 wt. %) $Ba_{1.03}Ce_{0.5}Zr_{0.4}Y_{0.1}O_{3-\delta}$ after sintering at 1300 ºC for 10 hours [34].

A significant densification of ~ 98% was achieved after sintering at 1400 ºC for 3 hours which is similar to the relative density of ~ 96% for $BaC_{0.5}Zr_{0.3}Y_{0.16}Zn_{0.04}O_{3-\delta}$ sintered at 1325 ºC for 10 hours [21]. The better densification might be due addition of ZnO as sintering aid into $BaZr_{0.3}Ce_{0.5}Y_{0.1}Yb_{0.1}O_{3-\delta}$ instead of ZnO doping at the B-site. Guo et al. [33] employed three methods for ZnO addition, sintering additive, in solution of nitrates and doping at the B site of $BaZr_{0.4}Ce_{0.4}Y_{0.2}O_{3-\delta}$ and found ZnO addition as the most effective method for getting better densification.

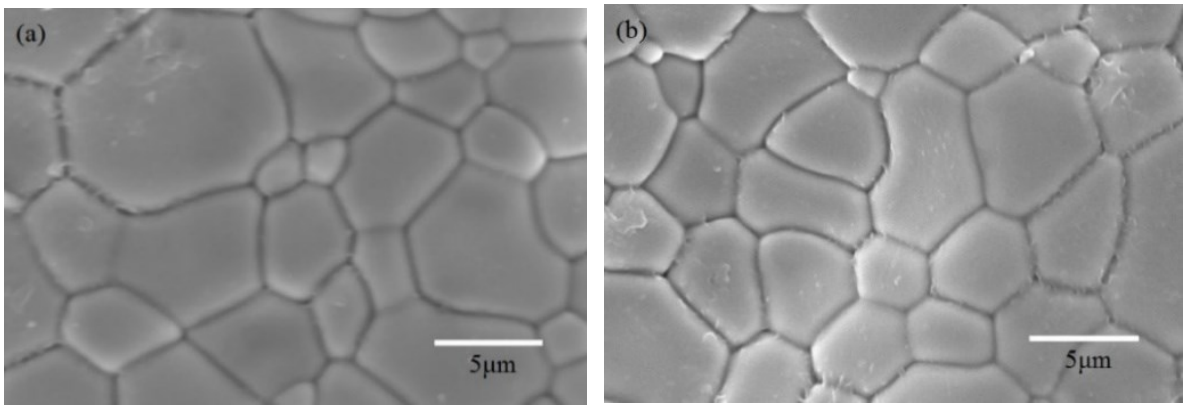

Fig. 3. SEM images of 1 wt. % in $BaZr_{0.3}Ce_{0.5}Y_{0.1}Yb_{0.1}O_{3-\delta}$ sintered at 1400 ºC for 3 hours.

3.4. Ionic Conductivity

Generally ionic conductivity in the range 10^{-2} – 10^{-3} S cm^{-1} at 600 ºC is required for practical applications of proton conducting oxides as electrolytes. Ionic conductivity, apart from its dependence on dopant concentration, synthesis history, strongly depends on microstructure as well. Ionic conductivities for 1 wt. % ZnO added $BaZr_{0.1}Ce_{0.7}Y_{0.1}Yb_{0.1}O_{3-\delta}$ along with three similar proton conducting electrolyte materials for comparison purposes, were measured in wet 5 vol% H_2/Ar atmosphere in order to avoid significant hole electronic contributions that would interfere if measured in air. Arrhenius plots for 1 wt. % ZnO added $BaZr_{0.1}Ce_{0.7}Y_{0.1}Yb_{0.1}O_{3-\delta}$ (curve 1), 1 wt. % ZnO added $BaZr_{0.3}Ce_{0.5}Y_{0.1}Yb_{0.1}O_{3-\delta}$ (curve 2), $BaCe_{0.5}Zr_{0.3}Y_{0.16}Zn_{0.04}O_{2-\delta}$ (curve 3), and $Ba_{0.5}Sr_{0.5}Ce_{0.6}Zr_{0.2}Gd_{0.2}Y_{0.2}O_3$ (curve 4) are shown in Fig. 4. Generally total ionic conductivities for

proton conducting oxides are measured at 600 ºC since up to this temperature the conductivity is pure protonic and above 600 ºC, there is contribution from oxide-ion conductivity as well. The ionic conductivity of 1 wt. % ZnO-added $BaZr_{0.3}Ce_{0.5}Y_{0.1}Yb_{0.1}O_{3-\delta}$ is 8.60 x 10^{-3} S cm^{-1} at 600 ºC which is close to the ionic conductivity values reported by Tao and Irvine [22] for $BaCe_{0.5}Zr_{0.3}Y_{0.16}Zn_{0.04}O_{2-\delta}$. The ionic conductivity value at 600 ºC is almost double to the reported conductivities for $BaCe_{0.5}Zr_{0.4}Y_{0.1}O_{3-\delta}$ or $BaCe_{0.3}Zr_{0.5}Y_{0.2}O_{3-\delta}$, which were 5 x 10^{-3} S cm^{-1} and 4.4 x 10^{-3} S cm^{-1} respectively [6], [18], [28]. It is much higher (about 4 times) than the reported conductivity value for $BaCe_{0.6}Zr_{0.3}Y_{0.1}O_{3-\delta}$ (2.33 x 10^{-3} S cm^{-1} at 600 ºC) under the same conditions [35]. Shi et al. [16] shows that the ionic conductivity of $BaZr_{0.3}Ce_{0.5}Y_{0.2-x}Yb_xO_{3-\delta}$ decreases with increasing Yb concentration. The observed conductivity with 10 mol% Yb dopant at the B site is higher than the compositions without Yb doping. This might be due to dense microstructure with bigger grain size.

The value of ionic conductivity at 600 ºC for ZnO-doped $BaZr_{0.3}Ce_{0.5}Y_{0.1}Yb_{0.1}O_{3-\delta}$ is even higher than the reported ionic conductivity ~ 7 x 10^{-3} S cm^{-1} for $BaZr_{0.3}Ce_{0.5}Y_{0.1}Yb_{0.1}O_{3-\delta}$ [16]. This shows that ZnO addition reduces the sintering temperature dramatically and at the same time is not detrimental to ionic conductivity. ZnO-added $BaZr_{0.3}Ce_{0.5}Y_{0.1}Yb_{0.1}O_3$ shows the activation energy (Ea) of 0.45 eV which is very close to the activation energy of pure $BaCe_{0.5}Zr_{0.3}Y_{0.2}O_{3-\delta}$ (Ea = 0.41 eV) [36].

The enhanced ionic conductivity is likely due to bigger grain size which is ~ 4 – 5 μm as shown in Fig. 3. As grain boundary resistance hinders total conductivity and an increase in grain reduces the grain boundary surface, which results in reduction of grain boundary resistance and consequently results an increase in ionic conductivity as observed by Fabbri et al. [28]. However, determination of individual conductivities for bulk and grain boundary conductivity will give better evidence.

After 600 ºC, the increase in ionic conductivity is not linear as can be seen from the inflexion noticed on the curve 2 in Fig 4. The mobility of protonic defects from experimental results as well as from quantum molecular dynamic (MD) simulations is believed to be due to dissociative adsorption of water in the presence of oxide vacancies [6], [37]–[39]. In Kroger-Vink notation the reaction is shown in Eq. 1.

$$H_2O_{(g)} + V_O^{\bullet\bullet} + O_O^x \rightarrow 2(OH)_O^{\bullet} \qquad (1)$$

Above 600 ºC the moisture content decreases, then protonic defects associated with OH ions also decreases and consequently total ionic conductivity decreases. That's why there is only slight increase in ionic conductivity after 600 ºC and at 700 ºC, a value ~ 9 x 10^{-3} S cm^{-1}, a slight increase from value of 8.60 x 10^{-3} S cm^{-1} at 600 ºC. This suggest p-type conduction mechanism as has been proposed for other proton conducting oxides [22].

Since ionic conductivity depends on many factors e.g. microstructure, material processing route, experimental parameters, purity level of precursors etc. So for confirmation it is better to compare its value with similar materials, processed from same starting precursors under the same processing conditions. For comparison studies, two other sample i.e. ZnO added $BaZr_{0.1}Ce_{0.7}Y_{0.1}Yb_{0.1}O_{3-\delta}$ and $BaCe_{0.5}Zr_{0.3}Y_{0.16}Z_{0.04}O_{3-\delta}$, from same precursors were processed and characterized under the same conditions and $Ba_{0.5}Sr_{0.5}Ce_{0.6}Zr_{0.2}Gd_{0.1}Y_{0.1}O_{3-\delta}$ (BSCZGY) was processed via wet chemical route. The measured conductivities of all four samples at 600 ^{o}C in wet 5 vol% H_2/Ar are shown in Table 2. The value of ionic conductivity for ZnO-added $BaZr_{0.3}Ce_{0.5}Y_{0.1}Yb_{0.1}O_{3-\delta}$ (curve 2) is higher than the ionic conductivity $BaCe_{0.5}Zr_{0.3}Y_{0.16}Zn_{0.04}O_{3-\delta}$ (curve 3) and that of $Ba_{0.5}Sr_{0.5}Ce_{0.6}Zr_{0.2}Gd_{0.2}Y_{0.2}O_{3-\delta}$ (curve 3) [40]. However, an ionic conductivity > 10^{-2} S cm^{-1} has been reported for $BaCe_{0.5}Zr_{0.3}Y_{0.16}Zn_{0.04}O_{3-\delta}$ [22]. The ionic conductivity of ZnO-added $BaZr_{0.3}Ce_{0.5}Y_{0.1}Yb_{0.1}O_{3-\delta}$ is comparable but slightly lower than that of ZnO-added $BaZr_{0.1}Ce_{0.7}Y_{0.1}Yb_{0.1}O_{3-\delta}$ (curve 1), which is obviously due to increased zirconia content in the former one. However, there is very big difference in chemical stability of both materials as evident from curve 1 and curve 4 in Fig. 4.

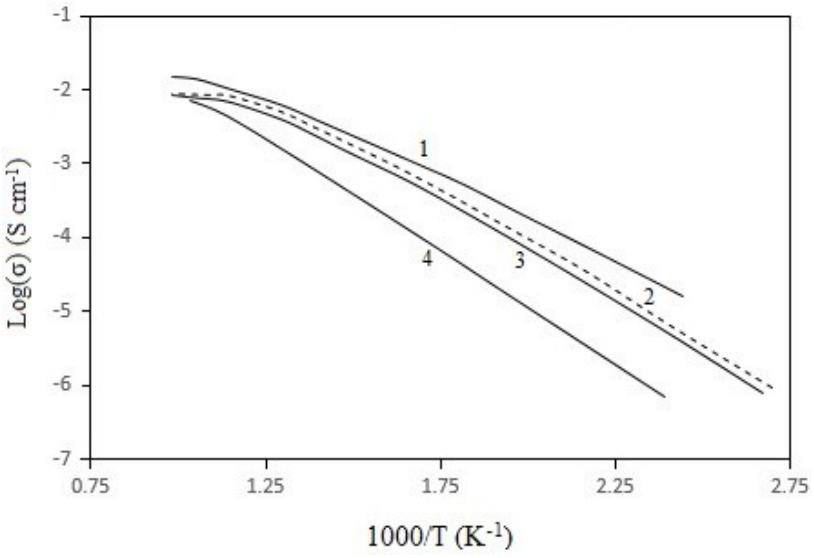

Fig. 4. Arrhenius plot. Curve:1 ZnO added $BaZr_{0.1}Ce_{0.7}Y_{0.1}Yb_{0.1}O_{3-\delta}$; curve 2: ZnO-added $BaZr_{0.3}Ce_{0.5}Y_{0.1}Yb_{0.1}O_{3-\delta}$; curve 3: $BaCe_{0.5}Zr_{0.3}Y_{0.16}Zn_{0.04}O_{2-\delta}$, curve 4: $Ba_{0.5}Sr_{0.5}Ce_{0.6}Zr_{0.2}Gd_{0.2}Y_{0.2}O_3$.

Table 2: Ionic conductivies of different compositions measured at 600 ºC in wet 5 vol% H_2/Ar atmosphere.

Composition	Ionic Conductivity (S cm^{-1})
1 wt. % ZnO-added $BaZr_{0.1}Ce_{0.7}Y_{0.1}Yb_{0.1}O_{3-\delta}$	~ 10^{-2}
1 wt. % ZnO-added $BaZr_{0.3}Ce_{0.5}Y_{0.1}Yb_{0.1}O_{3-\delta}$	8.6 x 10^{-3}
$BaZr_{0.3}Ce_{0.5}Y_{0.16}Zn_{0.04}O_{3-\delta}$	7 x 10^{-3}
$Ba_{0.5}Sr_{0.5}Ce_{0.6}Zr_{0.2}Gd_{0.1}Y_{0.1}O_{3-\delta}$	~4.5 x 10^{-3}

3.5. Chemical Stability

One of the main challenges of cerium-based proton conducting electrolyte materials is its stability issue in CO_2 containing atmospheres. It reacts with CO_2 and forms barium carbonate and ceria as shown in Eq. 2.

$$BaCeO_3 + CO_2 \rightarrow BaCO_3 + CeO_2 \quad (2)$$

The reactions in equation 2 occurs at 1141 ºC, that's why for testing chemical stabilities thermogravimetric analysis for all samples were carried out up to 1200 ºC in pure CO_2 [41]. Powder samples were heated in pure in CO_2 up to 1200 ºC with a heating rate of 3 ºC/min, held isothermally for 30 minutes at 1200 ºC and then cooled down to room temperature with a cooling rate of 3 ºC/min. The flow rate of CO_2 was 40 ml/min.

For comparison purpose, TGA of $BaZr_{0.3}Ce_{0.5}Y_{0.1}Yb_{0.1}O_{3-\delta}$, ZnO-added $BaZr_{0.3}Ce_{0.5}Y_{0.1}Yb_{0.1}O_{3-\delta}$, ZnO-added $BaZr_{0.1}Ce_{0.7}Y_{0.1}Yb_{0.1}O_{3-\delta}$ and $Ba_{0.5}Sr_{0.5}Ce_{0.6}Zr_{0.2}Gd_{0.1}Y_{0.1}O_{3-\delta}$ (BSCZGY) were also carried out under the same conditions (Fig. 5). BSCZGY proton conducting electrolyte material has more recently been reported for its excellent chemical stability [35]. However, ZnO-added $BaZr_{0.3}Ce_{0.5}Y_{0.1}Yb_{0.1}O_{3-\delta}$ was found the most stable among all compositions as shown in Fig. 5. XRD of ZnO-added $BaZr_{0.3}Ce_{0.5}Y_{0.1}Yb_{0.1}O_{3-\delta}$ before and after CO_2 exposure is shown in Fig. 6. No additional peak or evidence of any carbonation was observed. The stability of $BaZr_{0.3}Ce_{0.5}Y_{0.1}Yb_{0.1}O_{3-\delta}$ was found to be much poorer than ZnO-added $BaZr_{0.3}Ce_{0.5}Y_{0.1}Yb_{0.1}O_{3-\delta}$, which is consistent with literature [22]. $BaZr_{0.3}Ce_{0.5}Y_{0.1}Yb_{0.1}O_{3-\delta}$ was found more stable than ZnO-added $BaZr_{0.1}Ce_{0.7}Y_{0.1}Yb_{0.1}O_{3-\delta}$, which is obviously due to higher zirconia content. Surprisingly ZnO-added $BaZr_{0.3}Ce_{0.5}Y_{0.1}Yb_{0.1}O_{3-\delta}$ was found more stable than BSCZGY, which has recently been reported to be highly stable [35]. **The weight change in the present sample was almost zero whereas in $Ba_{0.5}Sr_{0.5}Ce_{0.6}Zr_{0.2}Gd_{0.1}Y_{0.1}O_{3-\delta}$ (curve 2), $BaZr_{0.3}Ce_{0.5}Y_{0.1}Yb_{0.1}O_{3-\delta}$ (curve 3) and ZnO-added $BaZr_{0.1}Ce_{0.7}Y_{0.1}Yb_{0.1}O_{3-\delta}$ (curve 4) the weight changes were about 0.35%, 1.6% and 4.2%, respectively.**

This might be due to a higher content of Zr in our composition and to the observed beneficial effect of ZnO addition to the stability of barium cerates, suppressing the surface carbonate formation for further reaction with Ba. The sintering aid added in this way aggregates even more over the BZ3C5YYb surface during the calcination and sintering, promoting the sintering of the BZ3C5YYb membrane and protecting it from intimate contact with CO_2.

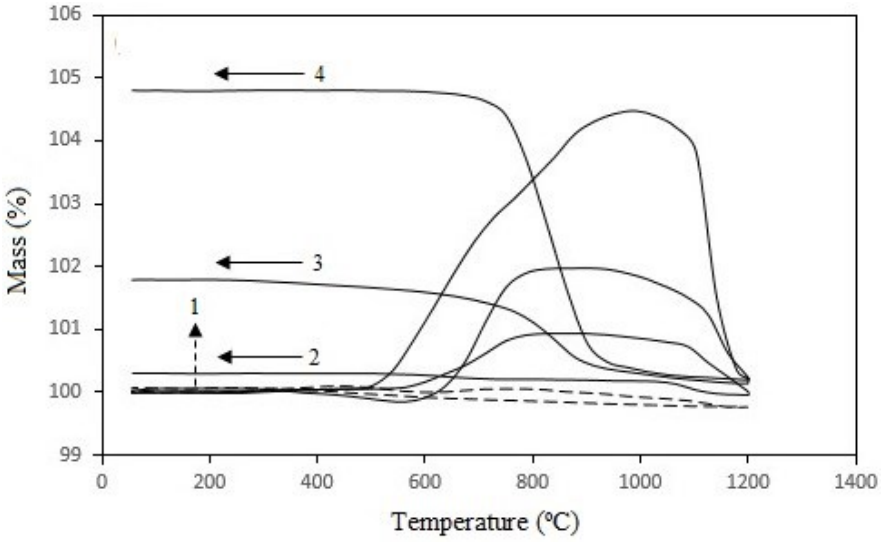

Fig. 5. TGA of samples in pure CO_2 heated up to 1200ºC with a heating rate of 3 ºC/min, isothermally held for 30 minutes and then cooled down at a rate of 3°C/min. **Each curves were given a number i.e.** ***curve 1*****: 1wt. % ZnO-added $BaZr_{0.3}Ce_{0.5}Y_{0.1}Yb_{0.1}O_{3-\delta}$ (present study),** ***curve 2*****: $Ba_{0.5}Sr_{0.5}Ce_{0.6}Zr_{0.2}Gd_{0.1}Y_{0.1}O_{3-\delta}$,** ***curve 3*****: $BaZr_{0.3}Ce_{0.5}Y_{0.1}Yb_{0.1}O_{3-\delta}$ and** ***curve 4*****: ZnO-added $BaZr_{0.1}Ce_{0.7}Y_{0.1}Yb_{0.1}O_{3-\delta}$.**

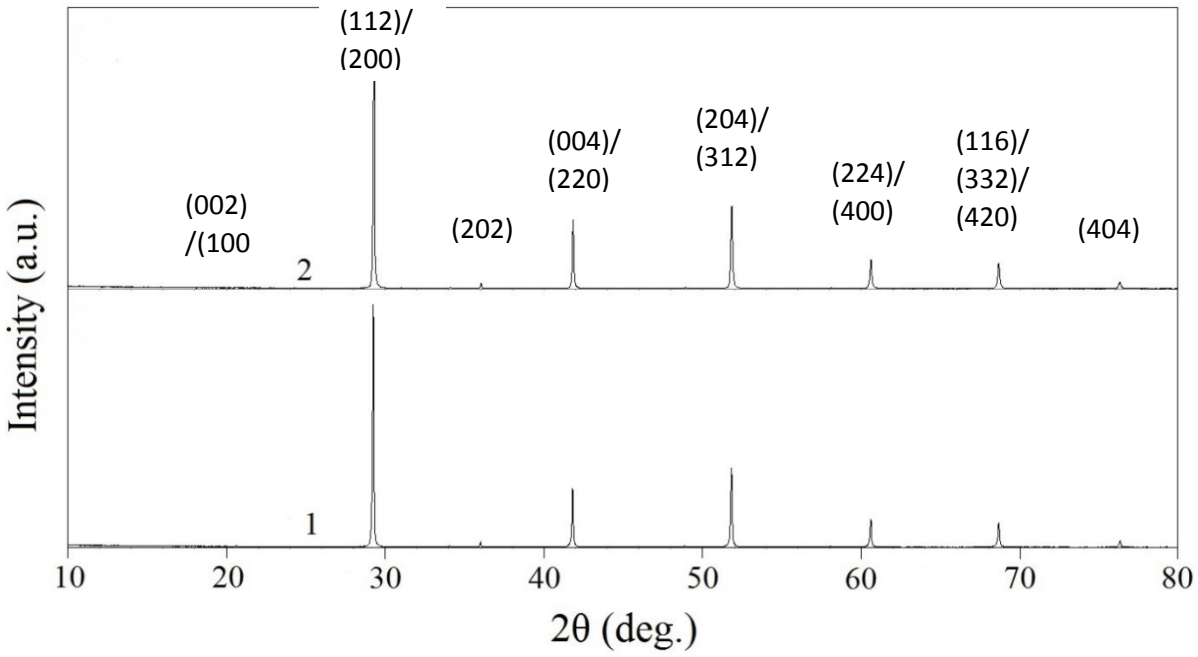

Fig. 6. XRD of (1) ZnO-added $BaZr_{0.3}Ce_{0.5}Y_{0.1}Yb_{0.1}O_{3-\delta}$ before stability test. (2) ZnO-added $BaZr_{0.3}Ce_{0.5}Y_{0.1}Yb_{0.1}O_{3-\delta}$ after stability test in pure CO_2 up to 1200ºC, held isothermally for 30 minutes and then cooled down at rate of 3ºC/min. Only prominent peaks are indexed in the figure.

3.6. Biaxial Flexure Strength

Flexure strength which is also known as modulus of rupture is a mechanical property which is commonly used to characterise ceramics. It is defined as the materials property to resist deformation under load. It can also be defined as the maximum stress in a biaxial mode needed to rupture the sample.

Generally functional properties of SOFCs components like ionic conductivity and chemical stability etc. are focused by researchers, however the mechanical strength is important as well for SOFCs components. As SOFC consists of anode, cathode, and electrolyte and even sometimes functional layers like anode-functional layer, so the SOFC should be able to withstand the stresses developed during its fabrication (co-sintering) process as well as during its operation, developed due to any mismatch of the thermal expansion co-efficient of the multi-layers. Also when many cells are combined to make a stack, sealant and interconnect materials become part of the stack and stresses can be developed from those components as well. It is therefore vital that SOFC components should have a certain level of mechanical strength for achieving required performance, reliability and durability.

Mechanical strength of the electrolyte material is perhaps more important than the other components in SOFCs. In case of Ni-based anode, the anode consists of 30 – 40 wt. % of electrolyte material. Apart from anode, cathode of H-SOFCs also consists about 30 wt. % of proton conducting electrolyte material. It is important to note that protonic conduction is also required for cathode material employed in Proton

Conducting SOFCs apart from MIEC (mixed ionic and electronic conduction) as required for oxide-ion SOFCs. There is no known cathode material yet which has well enough protonic conductivity as well as MIEC; this is why mostly composite cathodes are employed for Proton Conducting SOFCs. Composite cathode generally consists ~ 30 wt. % of electrolyte material which enhances triple phase boundary (TBP) and consequently results in better performance.

The formula [42] used for the measurement of biaxial strength is given in Eq. 3.

$$\sigma = -\frac{3}{4\pi}\frac{P}{t^2}(X - Y) \quad (3)$$

where σ = maximum centre tensile stress in mega Pascal (MPa), P = total load causing fracture in newton's.

and X and Y are given by Eq. 4 and 5.

$$X = (1 + \nu)\ln\frac{b^2}{a^2} + \frac{1-\nu}{2}\frac{b^2}{c^2} \quad (4)$$

$$Y = (1 + \nu)\left(1 + ln\frac{a^2}{c^2}\right) + (1 - \nu)\frac{a^2}{c^2} \quad (5)$$

where,

ν = Poisson's ratio, a = radius of support ring (m), b = radius of loaded area (m)

c = radius of the specimen (m), t = thickness of the specimen of fracture origin (m)

For the Lloyd LRX -05 fitted with a 500N load cell used where ν = 0.24, a = 4mm (4 x 10^{-3} m) and b = 0.36mm (0.36 x 10^{-3} m). These values have been used along with specimen details for the calculations of biaxial flexure strength.

The results of biaxial flexure strength for ZnO-added BZCYYb and ZnO-added BZ3C5YYb are potted in Figure 7. The average value of biaxial flexure strength for ZnO-added $BaZr_{0.3}Ce_{0.5}Y_{0.1}Yb_{0.1}O_{3-\delta}$ is in the range 100 – 200MPa, which is roughly 4 – 5 times higher than the flexure strength value for ZnO-added $BaZr_{0.1}Ce_{0.7}Y_{0.1}Yb_{0.1}O_{3-\delta}$, with biaxial flexure strength value in the range 20 – 40 MPa. The measured biaxial strength value is close to that of GDC (gadolinia doped-ceria), a well-known and useful oxygen ion conducting electrolyte material for SOFCs, with strengths between 150 – 175 MPa. To the best of our knowledge, there is not a lot of literature on the biaxial flexure strengths of proton conducting electrolyte materials.

3.7. Weibull Moduli of Biaxial Flexure Strength

Weibull moduli is a dimensionless quantity which is used to describe the variation in strength of brittle materials. This is related to the presence of flaws inside brittle materials since failure process starts from the weak points. Weibull plots of biaxial flexure strength for both samples are shown in Fig. 7; *pf* in $\ln(\ln\left(\frac{1}{1-pf}\right))$ (y-ordinate) means probability of failure.

For ZnO-added BZCYYb, Weibull moduli is in the range 3 – 4.5 and for ZnO - added BZ3C5YYb, it is in the range of 4.5 – 5.5 as can be seen from Fig. 7. Weibull moduli for ZnO-added BZ3C5YYb is comparable to the reported Weibull moduli value for YSZ (the most widely used electrolyte material for oxide-ion conducting SOFCs), which was in the range 5.4 – 6.2 [43], [44].

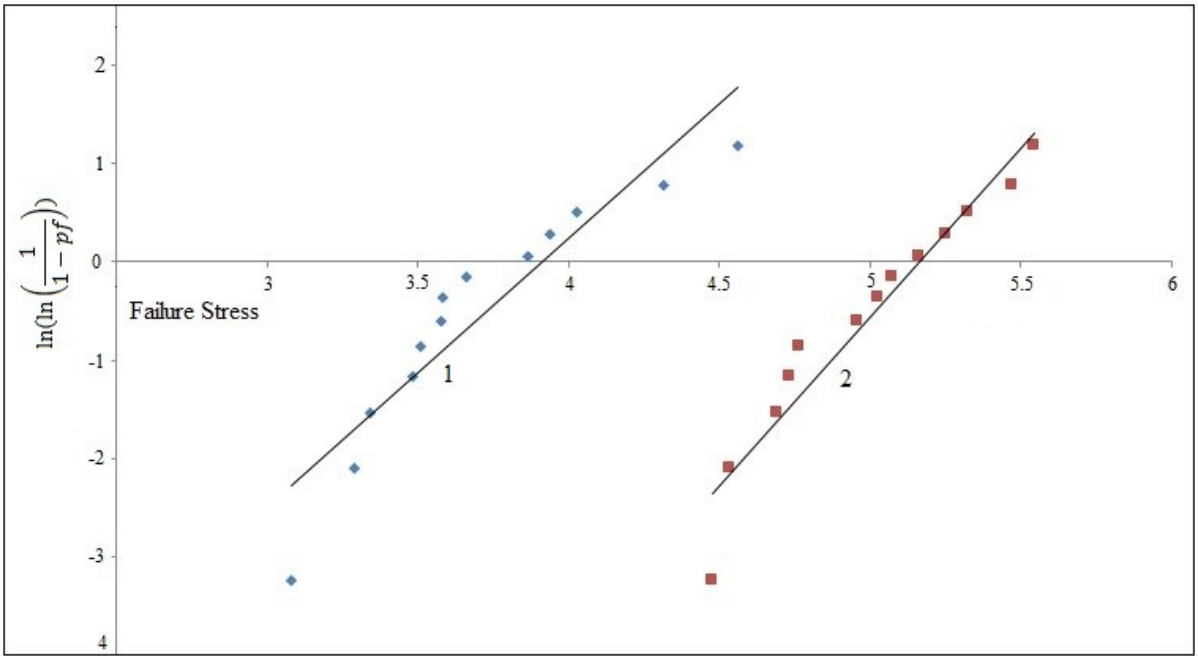

Fig. 7. Weibull plot of biaxial flexure strength for, (1) ZnO-added $BaZr_{0.1}Ce_{0.7}Y_{0.1}Yb_{0.1}O_{3-\delta}$ and (2) ZnO-added $BaZr_{0.3}Ce_{0.5}Y_{0.1}Yb_{0.1}O_{3-\delta}$, both sintered at 1400 ºC for 3 hours.

Conclusion:

ZnO-added $BaZr_{0.3}Ce_{0.5}Y_{0.1}Yb_{0.1}O_{3-\delta}$ show the tetragonal structure in the I4/mcm space group. In this study we have achieved single phase material with good ionic conductivity, high chemical stability and good sinterability simultaneously as well as high mechanical strength. These properties are very important for practical applications for proton conducting oxides. We observed an ionic conductivity of 8.60 x 10^{-3} S cm^{-1} at 600°C with very high chemical stability in pure CO_2 atmosphere and good sinterability. The material was highly dense ~ 98% at 1400 °C. Therefore, we understand that ZnO-added $BaZr_{0.3}Ce_{0.5}Y_{0.1}Yb_{0.1}O_{3-\delta}$ is a promising electrolyte material for Proton Conducting Solid Oxide

Fuel Cells (H-SOFCs) possessing good mechanical strength as well for anode-supported cells, which is not often reported.

Acknowledgements

The authors are grateful for the financial help from the S & T grant no.17. They a lot grateful to the help and cooperation from JTSI research group, School of Chemistry, University of St-Andrews. One of the authors, M Naeem Khan, is grateful for the Graduate Research Fellowship of Universiti Brunei Darussalam.

References

[1] E. Fabbri, L. Bi, J. L. M. Rupp, D. Pergolesi, and E. Traversa, "Electrode tailoring improves the intermediate temperature performance of solid oxide fuel cells based on a Y and Pr co-doped barium zirconate proton conducting electrolyte," *RSC Adv.*, vol. 1, no. 7, pp. 1183–1186, 2011.

[2] N. Radenahmad, A. Afif, P. I. Petra, S. M. H. Rahman, S.-G. Eriksson, and A. K. Azad, "Proton-conducting electrolytes for direct methanol and direct urea fuel cells – A state-of-the-art review," *Renew. Sustain. Energy Rev.*, vol. 57, pp. 1347–1358, May 2016.

[3] C. Duan, J. Tong, M. Shang, S. Nikodemski, M. Sanders, S. Ricote, A. Almansoori, and R. O'Hayre, "Readily processed protonic ceramic fuel cells with high performance at low temperatures," *Sci.* , vol. 349, no. 6254, pp. 1321–1326, Sep. 2015.

[4] T. Norby, "The promise of protonics," *Nature*, vol. 410, no. 6831, pp. 877–878, Apr. 2001.

[5] Y. Yamazaki, F. Blanc, Y. Okuyama, L. Buannic, J. C. Lucio-Vega, C. P. Grey, and S. M. Haile, "Proton trapping in yttrium-doped barium zirconate," *Nat Mater*, vol. 12, no. 7, pp. 647–651, Jul. 2013.

[6] E. Fabbri, D. Pergolesi, and E. Traversa, "Materials challenges toward proton-conducting oxide fuel cells: a critical review," *Chem. Soc. Rev.*, vol. 39, no. 11, pp. 4355–4369, 2010.

[7] D. Medvedev, A. Murashkina, E. Pikalova, A. Demin, A. Podias, and P. Tsiakaras, "BaCeO3: Materials development, properties and application," *Prog. Mater. Sci.*, vol. 60, pp. 72–129, Mar. 2014.

[8] **H. Iwahara, T. Esaka, H. Uchida, and N. Maeda**, "Proton conduction in sintered oxides and its application to steam electrolysis for hydrogen production," *Solid State Ionics*, vol. 3–4, pp. 359–363, Aug. 1981.

[9] K. D. Kreuer, "Proton -Conducting Oxides," *Annual Review of Materials Research*, vol. 33, no. 1. pp. 333–359, 2003.

[10] A. K. Azad, A. Kruth, and J. T. S. Irvine, "Influence of atmosphere on redox structure of BaCe 0.9 Y 0.1 O 2.95--Insight from neutron diffraction study," *Int. J. Hydrogen Energy*, vol. 39, no. 24, pp. 12804–12811, 2014.

[11] C. Zuo, S. Zha, M. Liu, M. Hatano, and M. Uchiyama, "Ba(Zr0.1Ce0.7Y0.2)O3–δ as an Electrolyte for Low-Temperature Solid-Oxide Fuel Cells," *Adv. Mater.*, vol. 18, no. 24, pp. 3318–3320, Dec. 2006.

[12] L. Bi, Z. Tao, C. Liu, W. Sun, H. Wang, and W. Liu, "Fabrication and characterization of easily sintered and stable anode-supported proton-conducting membranes," *J. Memb. Sci.*, vol.

336, pp. 1–6, 2009.

[13] L. Yang, S. Wang, K. Blinn, M. Liu, Z. Liu, Z. Cheng, and M. Liu, “Enhanced Sulfur and Coking Tolerance of a Mixed Ion Conductor for SOFCs: BaZr0.1Ce0.7Y0.2–xYbxO3–δ,” *Sci.* , vol. 326, no. 5949, pp. 126–129, Oct. 2009.

[14] Y. Liu, L. Yang, M. Liu, Z. Tang, and M. Liu, “Enhanced sinterability of BaZr0.1Ce0.7Y0.1Yb0.1O3−δ by addition of nickel oxide,” *J. Power Sources*, vol. 196, no. 23, pp. 9980–9984, 2011.

[15] L. Yang, S. Wang, K. Blinn, M. Liu, Z. Liu, Z. Cheng, and M. Liu, “Enhanced sulfur and coking tolerance of a mixed ion conductor for SOFCs: BaZr(0.1)Ce(0.7)Y(0.2-x)Yb(x)O(3-delta).,” *Science*, vol. 326, no. 5949, pp. 126–129, 2009.

[16] Z. Shi, W. Sun, and W. Liu, “Synthesis and characterization of BaZr0.3Ce0.5Y0.2−xYbxO3−δ proton conductor for solid oxide fuel cells,” *J. Power Sources*, vol. 245, pp. 953–957, Jan. 2014.

[17] B. Mirfakhraei, F. Ramezanipour, S. Paulson, V. Birss, and V. Thangadurai, “Effect of Sintering Temperature on Microstructure, Chemical Stability, and Electrical Properties of Transition Metal or Yb-Doped BaZr0.1Ce0.7Y0.1M0.1O3−δ (M = Fe, Ni, Co, and Yb),” *Front. Energy Res.*, vol. 2, p. 9, 2014.

[18] K. Katahira, Y. Kohchi, T. Shimura, and H. Iwahara, “Protonic conduction in Zr-substituted BaCeO3,” *Solid State Ionics*, vol. 138, no. 1–2, pp. 91–98, 2000.

[19] A. K. Azad and J. T. S. Irvine, “Synthesis, chemical stability and proton conductivity of the perovksites Ba(Ce,Zr)1-x Scx O3 - **d**,” *Solid State Ionics*, vol. 178, no. 7–10, pp. 635–640, 2007.

[20] P. Babilo and S. M. Haile, “Enhanced sintering of yttrium-doped barium zirconate by addition of ZnO,” *J. Am. Ceram. Soc.*, vol. 88, no. 9, pp. 2362–2368, 2005.

[21] E. Gorbova, V. Maragou, D. Medvedev, A. Demin, and P. Tsiakaras, “Investigation of the protonic conduction in Sm doped BaCeO3,” *J. Power Sources*, vol. 181, no. 2, pp. 207–213, 2008.

[22] S. Tao and J. T. S. Irvine, “A stable, easily sintered proton-conducting oxide electrolyte for moderate-temperature fuel cells and electrolyzers,” *Adv. Mater.*, vol. 18, no. 12, pp. 1581–1584, 2006.

[23] Y. Li, R. Guo, C. Wang, Y. Liu, Z. Shao, J. An, and C. Liu, “Stable and easily sintered BaCe0.5Zr0.3Y0.2O3−δ electrolytes using ZnO and Na2CO3 additives for protonic oxide fuel cells,” *Electrochim. Acta*, vol. 95, pp. 95–101, 2013.

[24] A. K. Azad, D. D. Y. Setsoafia, L. C. Ming, and P. M. I. Petra, “Synthesis and characterization of high density and low temperature sintered proton conductor BaCe0.5Zr0.35In0.1Zn0.05O3-d,” *Adv. Mater. Res.*, vol. 1098, pp. 104–109, 2015.

[25] A. K. Azad and J. T. S. Irvine, “High density and low temperature sintered proton conductor BaCe 0.5Zr0.35Sc0.1Zn0.05O 3-**d**,” *Solid State Ionics*, vol. 179, no. 19–20, pp. 678–682, 2008.

[26] D. A. Stevenson, N. Jiang, R. M. Buchanan, and F. E. G. Henn, “Characterization of Gd, Yb and Nd doped barium cerates as proton conductors,” *Solid State Ionics*, vol. 62, no. 3–4, pp. 279–285, 1993.

[27] J. Rodriguez-Carvajal, “Recent advances in magnetic structure determination by neutron powder diffraction + FullProf,” *Phys. B Condens. Matter*, vol. 192, no. 1--2, p. Pages--55, 1993.

[28] E. Fabbri, A. D'Epifanio, E. Di Bartolomeo, S. Licoccia, and E. Traversa, "Tailoring the chemical stability of Ba(Ce0.8-xZrx)Y0.2O3-delta protonic conductors for Intermediate Temperature Solid Oxide Fuel Cells (IT-SOFCs)," *Solid State Ionics*, vol. 179, no. 15–16, pp. 558–564, 2008.

[29] Y. Guo, Y. Lin, R. Ran, and Z. Shao, "Zirconium doping effect on the performance of proton-conducting BaZryCe0.8−yY0.2O3−δ (0.0≤y≤0.8) for fuel cell applications," *J. Power Sources*, vol. 193, no. 2, pp. 400–407, 2009.

[30] P. Sawant, S. Varma, B. N. Wani, and S. R. Bharadwaj, "Synthesis, stability and conductivity of BaCe0.8−xZrxY0.2O3−δ as electrolyte for proton conducting SOFC," *Int. J. Hydrogen Energy*, vol. 37, no. 4, pp. 3848–3856, 2012.

[31] A. K. Azad, C. Savaniu, S. Tao, S. Duval, P. Holtappels, R. M. Ibberson, and J. T. S. Irvine, "Structural origins of the differing grain conductivity values in BaZr0.9Y0.1O2.95 and indication of novel approach to counter defect association," *J. Mater. Chem.*, vol. 18, no. 29, p. 3414, 2008.

[32] S. Tao and J. T. S. Irvine, "Conductivity studies of dense yttrium-doped BaZrO3 sintered at 1325 **ºC**," *J. Solid State Chem.*, vol. 180, no. 12, pp. 3493–3503, 2007.

[33] Y. Guo, R. Ran, and Z. Shao, "Optimizing the modification method of zinc-enhanced sintering of BaZr 0.4Ce0.4Y0.2O3-δ-based electrolytes for application in an anode-supported protonic solid oxide fuel cell," *Int. J. Hydrogen Energy*, vol. 35, no. 11, pp. 5611–5620, 2010.

[34] C. Zhang, H. Zhao, N. Xu, X. Li, and N. Chen, "Influence of ZnO addition on the properties of high temperature proton conductor Ba1.03Ce0.5Zr0.4Y0.1O3−δ synthesized via citrate–nitrate method," *Int. J. Hydrogen Energy*, vol. 34, no. 6, pp. 2739–2746, 2009.

[35] J. Lv, L. Wang, D. Lei, H. Guo, and R. V Kumar, "Sintering, chemical stability and electrical conductivity of the perovskite proton conductors BaCe0.45Zr0.45M0.1O3−δ (M = In, Y, Gd, Sm)," *J. Alloys Compd.*, vol. 467, no. 1–2, pp. 376–382, 2009.

[36] Z. Shi, W. Sun, Z. Wang, J. Qian, and W. Liu, "Samarium and yttrium codoped BaCeO3 proton conductor with improved sinterability and higher electrical conductivity," *ACS Appl. Mater. Interfaces*, vol. 6, no. 7, pp. 5175–5182, 2014.

[37] S. Ricote, N. Bonanos, and G. Caboche, "Water vapour solubility and conductivity study of the proton conductor BaCe(0.9 − x)ZrxY0.1O(3 − δ)," *Solid State Ionics*, vol. 180, no. 14–16, pp. 990–997, 2009.

[38] H. Uchida, N. Maeda, and H. Iwahara, "Relation between proton and hole conduction in SrCeO3-based solid electrolytes under water-containing atmospheres at high temperatures," *Solid State Ionics*, vol. 11, no. 2, pp. 117–124, 1983.

[39] **W. Lee, A. Nowick, and L. Boatner**, "Protonic conduction in acceptor-doped KTaO3 crystals," *Solid State Ionics*, vol. 18–19, pp. 989–993, Jan. 1986.

[40] L. Malavasi, C. A. J. Fisher, and M. S. Islam, "Oxide-ion and proton conducting electrolyte materials for clean energy applications: structural and mechanistic features," *Chem. Soc. Rev.*, vol. 39, no. 11, pp. 4370–4387, 2010.

[41] R. Kannan, K. Singh, S. Gill, T. Fürstenhaupt, and V. Thangadurai, "Chemically stable proton conducting doped $BaCeO_3$ -no more fear to SOFC wastes.," *Sci. Rep.*, vol. 3, p. 2138, 2013.

[42] H. Matsumoto, Y. Kawasaki, N. Ito, M. Enoki, and T. Ishihara, "Relation Between Electrical Conductivity and Chemical Stability of BaCeO3-Based Proton Conductors with Different Trivalent Dopants," *Electrochem. Solid-State Lett.* , vol. 10, no. 4, pp. B77–B80, Apr. 2007.

[43] K. R. Reddy and K. Karan, "Sinterability, Mechanical, Microstructural, and Electrical

Properties of Gadolinium-Doped Ceria Electrolyte for Low-Temperature Solid Oxide Fuel Cells," *J. Electroceramics*, vol. 15, no. 1, pp. 45–56, 2005.

[44] A. Atkinson and A. Selçuk, "Mechanical behaviour of ceramic oxygen ion-conducting membranes," *Solid State Ionics*, vol. 134, no. 1–2, pp. 59–66, 2000.